NJC

Accepted Manuscript

This is an *Accepted Manuscript*, which has been through the Royal Society of Chemistry peer review process and has been accepted for publication.

Accepted Manuscripts are published online shortly after acceptance, before technical editing, formatting and proof reading. Using this free service, authors can make their results available to the community, in citable form, before we publish the edited article. We will replace this *Accepted Manuscript* with the edited and formatted *Advance Article* as soon as it is available.

You can find more information about *Accepted Manuscripts* in the Information for Authors.

Please note that technical editing may introduce minor changes to the text and/or graphics, which may alter content. The journal's standard Terms & Conditions and the Ethical guidelines still apply. In no event shall the Royal Society of Chemistry be held responsible for any errors or omissions in this *Accepted Manuscript* or any consequences arising from the use of any information it contains.

ROYAL SOCIETY OF CHEMISTRY

www.rsc.org/njc

Silver nanoparticles: green synthesis, self-assembly nanostructure and its application as SERS substrate

Elias de Barros Santos,[a*] Natiara Vaughn Madalossi [a], Fernando Aparecido Sigoli[a] and Italo Odone Mazali[a]*

[a]*Functional Materials Laboratory – Institute of Chemistry – University of Campinas - UNICAMP, P.O. Box 6154, Zip Code 13083-970 - Campinas - SP- Brazil*

* Authors to whom correspondence should be addressed.

E-mail: mazali@iqm.unicamp.br and eliasbarsan@gmail.com

Phone: +55 19 35213164 / Fax: +55 19 35213023

Silver nanoparticles: green synthesis, self-assembly nanostructure and its application as SERS substrate

Abstract

In this paper, silver nanoparticles were synthesized using citrus peel extracts such as *Citrus sinensis* (orange fruit, AgNP-Ora), *Citrus reticulata* (tangerine fruit, AgNP-Tan), and *Citrus aurantiflora* (lemon fruit, AgNP-Lem). The absorption spectra of the AgNP-Ora and AgNP-Tan colloids show localized surface plasmon band (LSPR) at 445 and 423 nm, respectively. For the same synthesis method, a low intensity of the LSPR band for AgNP-Lem is observed, indicating a low yield of this reaction. However, the transmission electron microscopy images show that the colloid prepared using lemon extract also presents AgNP larger than 5 nm (5 - 55 nm), which exhibit plasmonic properties. The synthesized silver nanoparticles are spherical-like shape and are highly crystalline, and they were self-assembled on NH_2-modified glass slides, obtained AgNP aggregates substrate for all three prepared silver colloids. We also explored the SERS activity of the AgNP substrates using 10^{-6} mol L^{-1} solutions of 4-aminebenzenethiol, rhodamine 6G, and methylene blue as Raman probe molecules. It was possible to detected with high signal-to-noise the SERS spectral pattern of all probe molecules on AgNP substrates. This simple, low cost, and greener method for synthesize silver nanoparticles may be valuable in future works about SERS sensors development and be extend to catalytic applications.

Keywords**:** Green synthesis, Ag nanoparticles, plasmonics properties, SERS activity.

1. Introduction

Silver nanoparticles have had a substantial impact across a diverse range of fields such as catalysis,[1,2] sensing,[3,4] metallic inks,[5,6] and medicine.[7,8] Silver has desirable physical properties, good relative abundance and low-cost, which make it an attractive material for several applications.[9] Also, it well known that silver nanoparticles have different optical and electromagnetic properties from its bulk material owing to quantum sizes and surface effects.[9,10] Recently, a large amount of works have been developed to study the optical properties of noble metal nanoparticles, including silver nanoparticles, which could support localized surface plasmon resonance (LSPR).[11-15] LSPR are electromagnetic modes associated with the excitation of collective oscillations of the electronic charge density in metals. The oscillation frequency is determined by some factors, such as density of electrons, electron mass, size and shape of the charge distribution in the nanostructure. Several unique properties can be achieved when adjusting the structure size, morphology, and composition of the metal nanoparticles, allowing to optimize the material for specific applications.[15-17] For example, LSPR excitations are the most important factor for generating strong optical fields in these nanostructures. Consequently, the materials that support LSPR can be used in surface-enhanced Raman scattering (SERS) studies and applications.

One of the most widely publicized metallic nanoparticles synthesis has been about silver.[9] Related to this, manufacturing and application of silver nanoparticles-based materials has become a very active field in materials science. Silver nanoparticles can be prepared by several methods including chemical reduction, electrochemical techniques, and photochemical reduction.[18-20] However, toxic compounds such as sodium borohydride are usually involved, some synthetic process are time consuming and/or present low-yield in silver nanoparticles formation.[9,10] Recently, several studies

has been focused on green nanoparticles synthesis approaches, including silver nanoparticles, to avoid hazardous materials.[21-25] Also, these eco-friendly synthetic approaches are based on use of plant extracts, which make these processes simple, low-cost effective, and efficiency produce a wide variety of shapes with sizes ranging from 1 to 100 nm. Basavegowda and Lee[26] described the use of *Satsuma mandarin* peel extract to the synthesis of silver nanoparticles. Dubey *et al.*[27] reported the use of fruit extract of *Tanacetrum vulgare* to synthesize silver and gold nanoparticles. Also, the use of plant extracts can be extend to synthesized others metals, such as copper nanoparticles as showed recently by Brumbaugh *et al.*[28]

By far, beside gold nanoparticles, silver nanoparticles are the most important material widely used as SERS substrate.[29] Silver nanoparticles have been extensively used owing to their unique optical properties, i.e., strong LSPR, that can be tuned in the visible range when varying size, morphology, composition, and aggregates formation.[30-33] Recently, a great deal of research effort has been devoted to transfer SERS into practical analytical applications. However, fabrication of SERS nanostructures with both high sensitivity and high reproducibility remains difficult.[29,34] Also, methods to produce low-cost substrates for practical application of SERS in routine laboratory analysis and on-site analysis in the field are even limited. In this context, silver nanoparticles synthesized using plant extracts have the potential to be a good alternative to add efficiency and low-cost in the same SERS substrate preparation.

Although a lot of research dealing with metallic silver nanoparticles synthesis using fruit and plant extracts have been published, to the best of our knowledge, the use of this nanoparticles in plasmonics and/or SERS studies has not been investigated so far. Therefore, the objective of this study was for the first time go beyond of the synthesis process. In other words, to synthesize silver nanoparticles using citric peel

extracts, to explore its plasmonics properties, and to investigate its SERS activity. For this purpose, citrus peel extracts from orange, tangerine, and lemon were used to synthesize silver nanoparticles without adding external surfactant and/or capping agent. These synthesized silver nanoparticles were self-assembled on glass slides and their SERS responses were explored using 4-aminobenzenethiol (4-ABT), rhodamine 6G (Rd6G), and methylene blue (MB) as Raman probe molecules. These model molecules were chosen because they are widely used as Raman probes in SERS studies.

2. Materials and methods

2.1. Chemicals

Silver nitrate (ACS grade), 3-aminopropyl-trimetoxisilane (APTMS), 4-aminobenzethiol (4-ABT), Rhodamine 6G (Rd6G), and methylene blue (MB) were purchased from Sigma Aldrich and used without purification. Ethylic alcohol (ACS grade), hydrogen peroxide, hydrochloric acid and sulfuric acid were purchased from Synth.

2.2. Preparation of citrus peel extracts and silver nanoparticles synthesis

The same procedure was used for the three different citrus peel extracts. Fresh orange (*Citrus sinensis*), tangerine (*Citrus reticulata*), and lemon (*Citrus aurantiflora*) fruits were purchased from a local supermarket in Campinas in São Paulo state, Brazil. These citric fruits were washed thoroughly with distilled water and their peels were incised into small pieces. The peels pieces (30 g) were weighed and transferred to three different 500 mL flasks containing 100 mL of deionized water, mixed, and boiled for 10 min. The citrus peel extracts obtained were filtered thorough Whatman No. 1 filter

paper and the filtered were collected in three different 250 mL Erlenmeyer flasks. The pH values of the peels extracts were measured using an Analyser digital pH-meter.

Silver nanoparticles synthesis: the same procedure was used for the three different citrus peel extracts. Briefly, 10 mL of citrus extract was mixed with 100 mL of aqueous solution of $AgNO_3$ 10^{-3} mol L^{-1} and stirred at 30 ^oC for 60 min. The as-synthesized silver nanoparticles were named AgNP-Ora (from orange extract), AgNP-Tan (from tangerine extract), and AgNP-Lem (from lemon extract).

2.3. Silver nanoparticles deposition onto glass slides

The functionalization of glass slides (1 cm x 1 cm) with APTMS for preparation of SERS substrates is described in previous work by our group.[35] Volumes of 100 µL of each kind of AgNP colloids were dropped onto NH_2-modified glass slides. Subsequently, the glass slides were placed into an oven to dry at 40 ^oC for 15 min. After this first deposition (1D substrates), the AgNP substrates were immersed in APTMS sol-gel for 20 min. After that, the substrates 1D were washed with deionized water and dried with N_2 flow. Subsequently, volumes of 100 µL of each AgNP colloids were dropped onto substrates 1D and they were placed into a oven to dry at 40 ^oC for 15 min. Finally, the substrates with two AgNP depositions (2D substrates) were washed with deionized water and dried with N_2 flow.

2.3. Materials characterization

UV-Vis spectra of the AgNP colloids were obtained using a spectrometer Agilent Cary probe 50. Fourier transform infrared (FTIR) spectra were acquired with a NICOLET 6700 FTIR. Samples were prepared for FTIR analysis by freeze-drying the aqueous citrus peel extracts, grinding the dried samples with KBr, and forming KBr

pellets. The AgNP 1D and 2D substrates scanning electron microscopy (SEM) images were obtained using Field Emission Gun microscope model Inspect, with acceleration voltage of 15 kV. Before analysis the samples were covered with a carbon thin film. Also, an energy-dispersive X-ray spectroscopy (EDS) elemental analysis were carried out for the AgNP substrates. High-resolution transmission electron microscopy (HRTEM) images were obtained using a JEOL JEM-3010 microscope (300 kV, 1.7 Å point resolution). The sample was prepared by drop-drying the colloidal AgNP solution on a holey carbon coated Cu grid.

2.4. SERS measurements

All measurements were accomplished using a confocal Jobin-Yvon T64000 Raman spectrometer system, equipped with a liquid N_2 cooled CCD detector and a microscope was used. The excitation source was a laser at 633 nm. The laser power at the sample surface was about 2.5 mW. The laser was focused with a 100x focal-lens objective to a spot of about 1 μm. For all measurements, the laser exposure time was dependent on the Raman probe molecule (10 s for 4-ABT and for Rd6G, and 5 s for MB). Aliquots of 25 μL of 10^{-6} mol L^{-1} 4-ABT, Rd6G or MB ethanollic solutions were dropped onto 2D AgNP substrates. After the solvent evaporation the substrates were ready to be analyzed.

3. Results and discussion

3.1. Synthesis and characterization of AgNP using citrus peel extracts

The green methods of silver nanoparticles synthesis using plants extracts were reported to be eco-friendly when compared to traditional chemical methods, since these greener procedures are free of added chemical compounds such as surfactants and

capping agents. Then, the first step here is understanding what are functional groups involved in the silver nanoparticles reduction and the nanoparticle chemical stability. The FTIR spectral pattern of the three lyophilized citrus peel extracts are similar to each other (Fig. 1). Also, the general features of the FTIR spectra are common to spectra of plant extracts reported elsewhere.[36-38] The broad band at 3404 cm^{-1} is assigned to −O−H stretch from hydroxyl groups expected to be present in the peel extracts, such as sugars and polyphenols. Although the extracts have been lyophilized, this band may also be a contribution from incorporated water molecules. There are several possible assigns for the band located at 1055, 2931 and its shoulder at 2869 cm^{-1} due to variety of N− and O−containing functional groups. Also, these bands may be a contribution of C−C stretch and C−H stretch from hydrocarbon chains. The band at 1609 cm^{-1} is assigned to amide I band from protein carbonyl stretch. Bands located at around 1419 cm^{-1} are attributed to C−O−H bending vibrations. As observed, the FTIR spectra of the citrus peel extracts indicate the presence of several functional groups, which can be associated with the presence of bioactive compounds such as flavonoids, citric acid, carotenoids, and aromatic compounds. Many of those compounds exhibit antioxidant properties, and consequently, can play important role as reducing and/or capping agents in nanoparticles synthesis.[39,40]

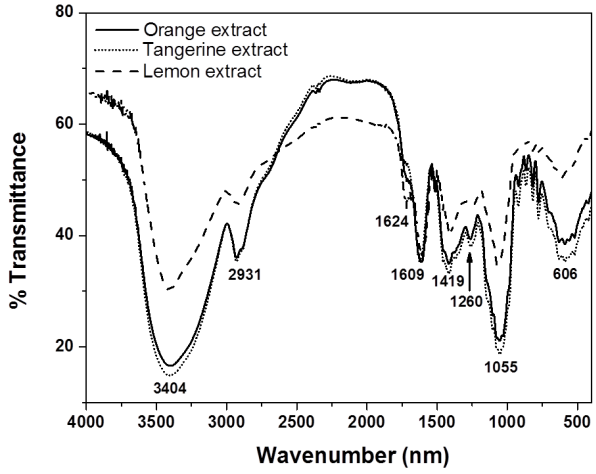

Figure 1. FTIR spectra of the lyophilized citrus peel extracts.

During the reaction process, the color of the solutions turned from light yellow to brown (AgNP-Ora), dark-red (AgNP-Tan), and yellow (AgNP-Lem) as shown in Supplementary material (Fig. SM1). UV-vis absorption spectra of the peel extracts and of the AgNP aqueous solutions were used to understanding the differences observed in the reaction process (Fig. 2). All UV-vis absorption spectra of the citrus peel extracts exhibit a similar pattern, showing absorption bands at 320 and at around 270 nm. For AgNP-Ora and AgNP-Tan is observed the absorption band at 445 and 423 nm, respectively, which is consistent with the localized surface plasmon band (LSPR) related to the formation of silver nanoparticles (Fig. 2(a) and (b)). However, it is observed a lack of LSPR band in the AgNP-Lem UV-vis spectrum (Fig. 2(c)), which suggests the formation of silver clusters and/or ultrasmall silver nanoparticles. Ultrasmall nanoparticles and atomically precise clusters lose their visible extinction features as a function of the size, being characterized for absorbing into the UV range.[41,42] The formation of ultrasmall silver nanoparticles and/or clusters consisting of small number of atoms, and their chemical stability in aqueous solution, was reported and discussed by Linnert *et al*.[42] The silver species such as Ag_4^+ and Ag_n clusters (n <

10 atoms) are commonly formed in many procedures of silver nanoparticles colloidal synthesis and the bands located at around 280 and 323 nm are associated with their formation (Fig. 2). Also, these bands may be a contribution of the peel extracts absorption. The ultrasmall AgNP, also named quasi-metallic particles, shows absorption at around 360 nm.[42] The silver particles which possess metallic properties presents absorption from 380 nm to visible range.

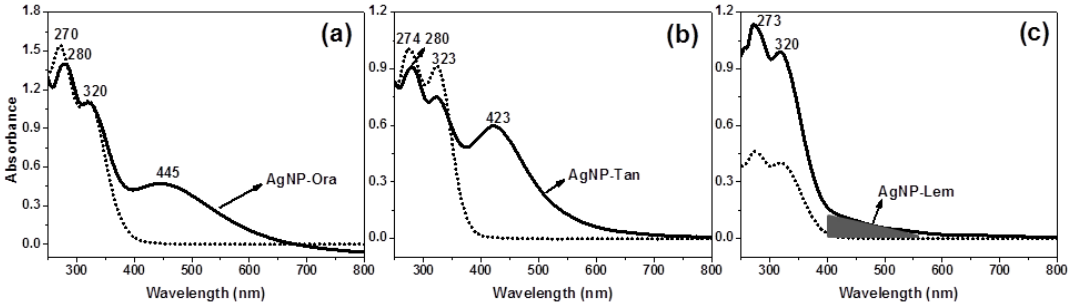

Figure 2. UV-vis spectra of the AgNP colloids (solid line) and of their respective citrus peel extract (point line) orange (a), tangerine (b), and lemon (c).

According to the FTIR data, the citrus peel extracts present the same chemical composition. However, the UV-vis result indicates that 60 min of the reaction time should not be enough to growing the silver nanoparticles when using the lemon peel extract. This can be explained according to pH values of the citrus peel extracts, which were 4.0 for lemon extract and 6.0 for orange and tangerine extracts. However, in the end of the reaction the pH values were 5.0 for AgNP-Lem, and 7.0 for AgNP-Ora and for AgNP-Tan. In other words, the lemon peel extract is more acidic than the orange and tangerine extracts. This result suggests that the amount of acidic molecules such as citric acid and ascorbic acid is highest for the lemon extract. This kind of molecules present a strong reducing power, and also, play roles of capping agents in nanoparticles synthesis.[43-45] Consequently, a high concentration of these molecules can easily to

224 reduce $Ag^{+}_{(aq)}$ ions in solution, forming small silver particles, which are rapidly capped
225 for those molecules. Although the lack of a defined LSPR band in the UV-vis
226 absorption spectrum of AgNP-Lem, it can be observed in Fig. 2(c), the gray area of the
227 spectrum, that the absorption between 400 and 550 nm is not zero. This result indicates
228 the formation of AgNP between 5 - 100 nm range as showed by HRTEM analysis (Fig.
229 3). However, the concentration of these silver nanoparticles should be lower than others
230 two citrus peel extracts, since a defined LSPR band was not observed in that UV-vis
231 spectrum.

232 Representatives HRTEM images of the silver nanoparticles colloids show the
233 formation of nanoparticles with average sizes of 31.0 ± 18.3 nm for AgNP-Ora, 29.8 ±
234 18.7 nm for AgNP-Tan, and 18.5 ± 11.6 nm for AgNP-lem (Fig. 3). All the samples
235 present AgNP with size below 5 nm, which are defined as ultrasmall nanoparticles[46] as
236 evidenced before by UV-vis analysis. Although the lack of a defined LSPR band at UV-
237 vis spectrum of the silver colloid prepared using lemon peel extract, the HRTEM
238 analysis shows the presence of the formation of AgNP-Lem until 55 nm. The majority
239 of the AgNP formed are spherical-like shape and are highly crystalline (Fig. SM2).
240

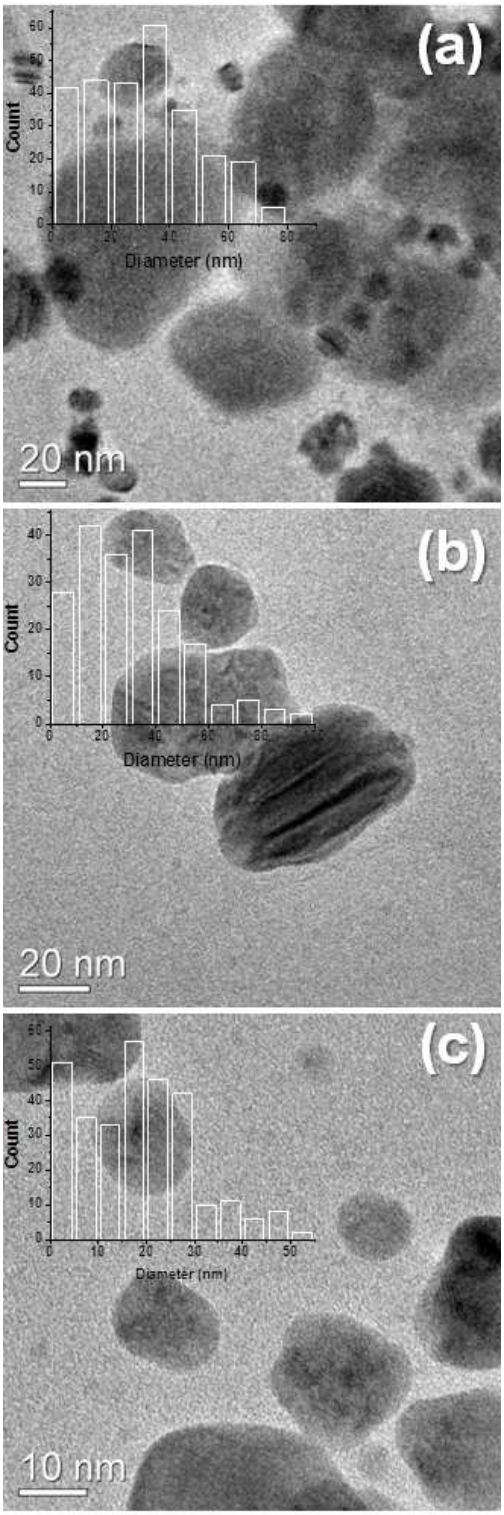

241

242 **Figure 3.** HRTEM images of the AgNP-Ora (a), AgNP-Tan (b), and AgNP-Lem (c).

243

Up to now, we have concluded that the same procedure to synthesize silver nanoparticles using citrus peel extracts resulted in the formation of AgNP with different size distributions due to the complexity of the chemical composition of the extracts. However, the colloids prepared contain high concentration of silver nanoparticles with preferential spherical symmetry. Also, the AgNP exhibit LSPR bands in the visible range, which is dependent on its size. These characteristics qualify the as-prepared AgNP to be used as SERS substrate. For example, using the laser line at 633 nm as source in Raman/SERS measurements the AgNP-Ora and AgNP-Tan seems to be the better samples than AgNP-Lem. As can be seen in Fig. 4, the last sample does not exhibit a defined LSPR band in the visible range, indicating an unfavorable condition to be used in SERS, where the laser line and surface plasmon coupling is important.[47] However, the others two samples exhibit LSPR bands near the line at 633 nm, which is a more appropriate condition for SERS. Although the AgNP prepared using lemon extract does not exhibit one defined LSPR band in visible range, the HRTEM analysis shows that there are silver nanoparticles with an adequate size to be tested in SERS. Then, the methodology of self-assembling AgNP was adopted to prepare the nanoparticles substrates for SERS as shown in Fig. 5.

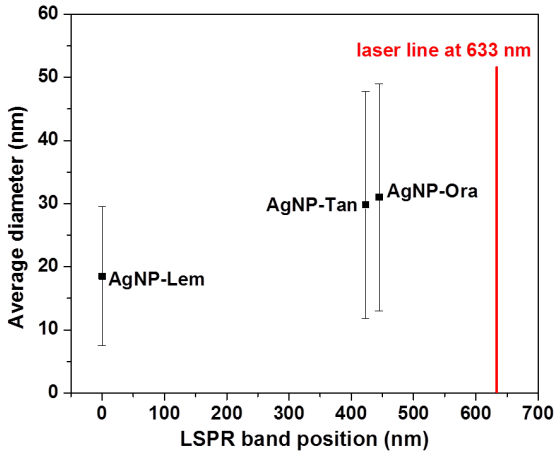

Figure 4. LSPR band position of the AgNP-Ora, AgNP-Tan, and AgNP-Lem as function of the average size and its position compared to the laser line at 633 nm.

3.2. Preparation of self-assembled AgNP substrates

The strategy of self-assembling plasmonic nanostructures has been employed with great success by many researches aiming to prepare efficient materials for specific applications.[48] For example, the organization of AgNP using APTMS sol gel molecules as linker offers a favorable condition for coupling surfaces plasmons of adjacent nanoparticles and enhancing the electric field in interparticle gaps (in the so-called "hot spots"). Due to hot spots generation and consequently amplification of Raman signals this approach has been employed for preparing SERS substrates.[49,50] In Fig. 5 is shown a representative scheme showing the strategy employed in the present work to prepare the self-assembled AgNP structures.

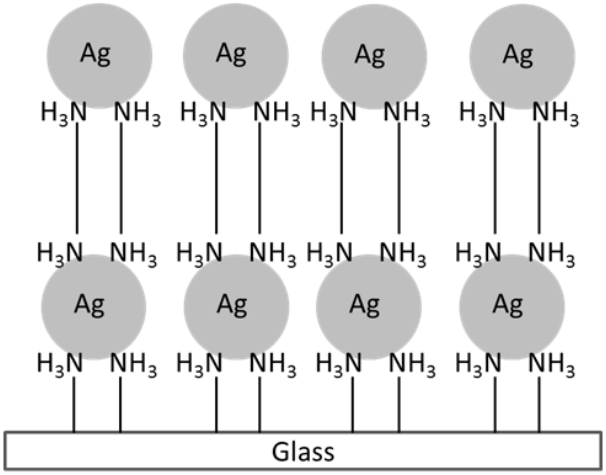

Figure 5. Representation of the bilayer AgNP structure on NH_2-modified glass slide. The APTMS sol gel molecules are the linker between the AgNP layers. Drawing out of scale, only for illustration.

Fig. 6 shows the SEM images of the AgNP substrates prepared with one deposition and two depositions of AgNP. As can be seen in Fig. 6, one deposition is not enough to cover the glass surface of AgNP as well as leads to formation of small AgNP aggregates, which are dispersed on glass surface. The AgNP-Lem 1D substrate presents few small aggregates comparing with other two 1D substrate due to its low concentration and/or small size of the AgNP in this colloid (Fig. 6(c)). As can be observed in Fig. 6 (images on the right side), after two depositions of AgNP, the aggregates are larger than before, forming rich areas of AgNP, even for the AgNP-Lem substrate. This result shows that the self-assembly strategy is efficient in the preparation of the AgNP substrate, promoting interparticle nanogaps generation and stability due the formation of chemical bonds between the AgNP and the available -NH_2 groups (Fig.5).

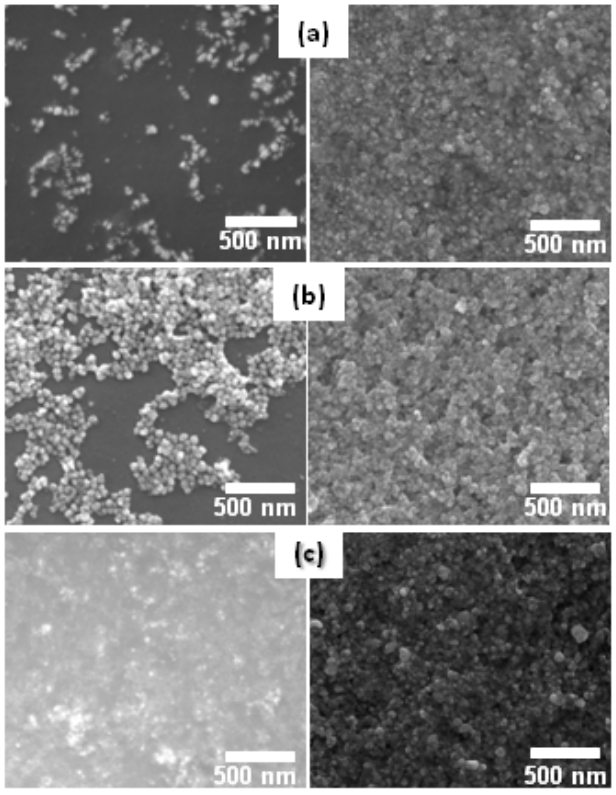

294 **Figure 6.** SEM images of the 1D substrates (left side) and 2D substrates (right side) for
295 AgNP-Ora (a), AgNP-Tan (b), and AgNP-Lem (c).
296
297 EDS elemental analysis data show the same elements composition for all three
298 AgNP 1D substrates (Fig. 7). The two peaks around 3.0 keV are characteristic of
299 metallic Ag, which are assigned to Ag-L_α and Ag-L_β lines. The difference of the
300 percentage of silver is related to the position where the EDS analysis was recorded on
301 the AgNP aggregates. Also, the high percentage of silver observed for the AgNP-Tan
302 1D substrate is in agreement with the SEM data, which showed the formation of larger
303 AgNP aggregates than the other two AgNP substrates. Carbon and oxygen are from the
304 organic compounds present in citrus peel extracts. Also, the oxygen signal may be a
305 contribution from the glass, used as support, as well as the other observed glass
306 components such as sodium, magnesium, silicon, and calcium.

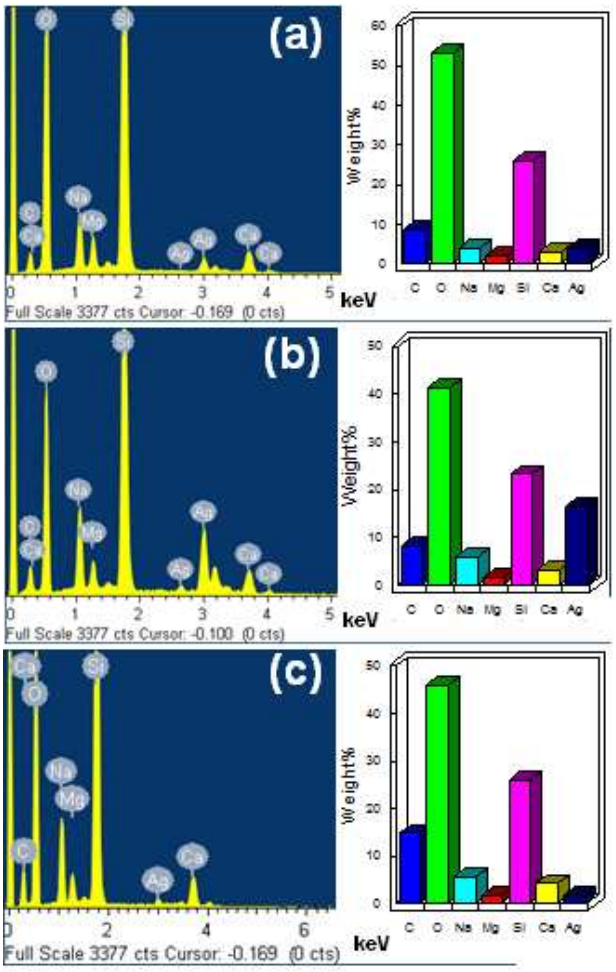

Figure 7. EDS data of the 1D substrates: AgNP-Ora (a), AgNP-Tan (b), and AgNP-Lem (c).

3.3. SERS activity of the AgNP 2D substrates

To evaluate the SERS activity of the AgNP 2D substrates 4-aminobenzenethiol, rhodamine 6G, and methylene blue were chosen as Raman probe molecules. As can be seen in Fig. 8, it is possible to detect the three molecules (10^{-6} mol L^{-1}) on AgNP-Ora substrates. It is not our intention here to discuss in detail all assignments for the bands in all SERS spectra. The main bands for 4-ABT (at 1070 cm^{-1} assigned to υ_{CS+CC}), MB (at 1615 cm^{-1} assigned to $\upsilon_{C=C}$), and Rd6G (at 1500 cm^{-1} assigned to $\upsilon_{C=C}$) are in agreement with previous works reported in the literature.[51-53] The most important issue

in this work is to show that the as-prepared AgNP, using citrus peel extracts, can be employed as efficiency in SERS, similar to the silver nanoparticles prepared by other synthetic approaches. However, the method reported here is simply, eco-friendly and cheap.

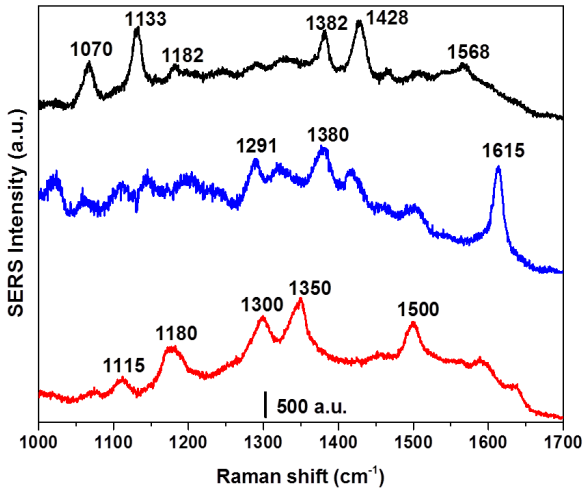

Figure 8. SERS spectra of 10^{-6} mol L^{-1} 4-ABT (black), MB (blue), and Rd6G (red) on AgNP-Ora substrates.

As can be visualized in Figs. 9 and 10, the substrates prepared using the AgNP-Tan or AgNP-Lem also exhibited SERS activity, being possible to detect the three molecules probe. For the AgNP-Tan substrate the signal-to-noise Raman signal from 4-ABT is higher than the Raman signal for the two dyes. A similar result is observed when analyzing the SERS spectra in Fig. 10 for AgNP-Lem, where can be observed a better quality in the SERS spectrum for 4-ABT. The main difference is the Rd6G SERS spectrum, where is not observed the band around 1500 cm^{-1}, as observed in Figs. 8 and 9. However, it can be observed a band at 1544 cm^{-1}, which also can be attributed to this molecule. This fluctuation of the position of some bands is commonly observed in

337 SERS studies, and it can be related to specific orientation of the probe molecule
338 adsorbed on substrate surface as well as single molecule behavior.[51-53]
339

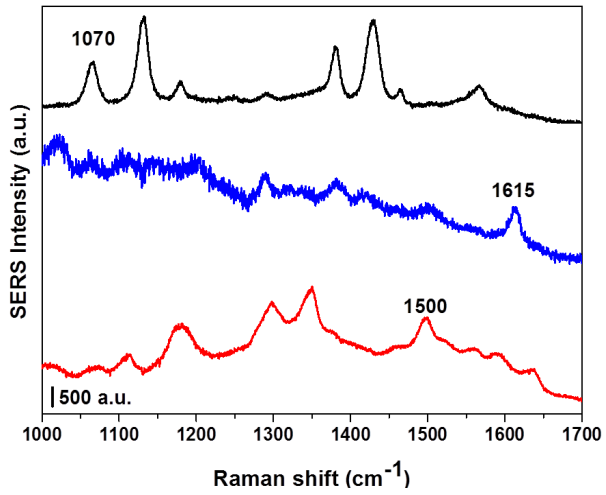

340
341 **Figure 9.** SERS spectra of 10^{-6} mol L^{-1} 4-ABT (black), MB (blue), and Rd6G (red) on
342 AgNP-Tan substrates.
343
344

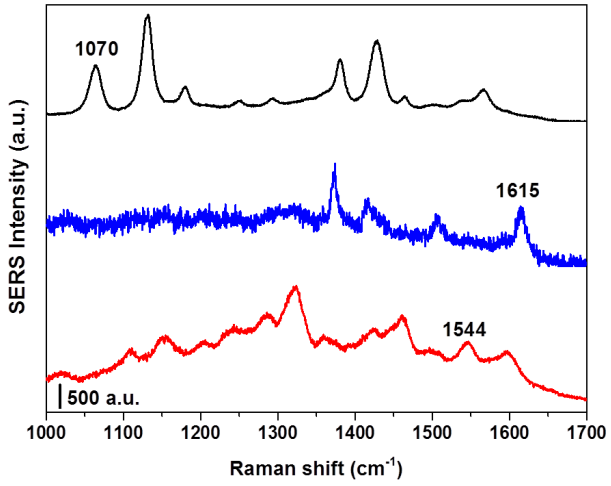

345
346 **Figure 10.** SERS spectra of 10^{-6} mol L^{-1} 4-ABT (black), MB (blue), and Rd6G (red) on
347 AgNP-Lem substrates.
348

One of the most interesting result here is the SERS activity of the AgNP-Lem substrate for the three Raman probe molecules. As discussed above, the as-prepared silver nanoparticles using the lemon extracts is lack in LSPR due the low yield of the reaction. However, the HRTEM images show the presence of silver nanoparticles larger than 5 nm, which posses plasmonic properties. This explains the SERS activity of the AgNP-Lem substrate. Also, other important aspect here is the strategy of using the self-assembly approach to prepare the AgNP substrates. When the particles are in close packed assembly, then the electromagnetic field influences its neighbor. Consequently, the oscillating electrons in one particle feel the electric field due to the oscillation of the second particle, which can lead to plasmon coupling and generation of collective plasmon oscillations of the aggregate structures.[48,54] The plasmon coupling is an important contribute to amplification of the optical and surface-enhanced Raman scattering signals. This explain the SERS activity of the all AgNP aggregates substrates and also, being extremely decisive for the AgNP-Lem substrate SERS activity.

4. Conclusions

In this work, we present a green synthesis approach to prepare silver nanoparticles using citrus peel extracts and their self-assembly on glass slides to be used as SERS substrate. The as-synthesized AgNP are stable and exhibit LSPR band at visible range. The nanoparticles were self-assembled onto amine-modified glass slides, forming AgNP aggregates substrates. Self-assembled substrates of AgNP-Ora, AgNP-Tan, and AgNP-Lem have been further tested for SERS of 4-ABT, MB, and Rd6G at 10^{-6} mol L^{-1} concentration. It was possible to detected with high signal-to-noise the SERS spectral pattern of all probe molecules for all the three AgNP substrates. Furthermore, the Raman results show that the SERS intensities for all AgNP substrates

374 are high when using 4-ABT probe molecule than the SERS intensities of the dyes probe.
375 This simple, low cost, and greener method for synthesize silver nanoparticles may be
376 valuable in SERS sensors development and can be extended for others fields such as
377 catalytic applications.
378
379 **Acknowledgments**
380 The authors would like to thank the FAPESP, CAPES and CNPq for financial supports.
381 Contributions from Multiuser Laboratory of Advanced Optical Spectroscopy
382 (LMEOA/IQ/UNICAMP) for Raman analysis and Brazilian Nanotechnology National
383 Laboratory (LNNano, Campinas-SP) for SEM and HRTEM analysis are also gratefully
384 acknowledgment. This is a contribution of the National Institute of Science and
385 Technology in Complex Functional Materials (CNPq-MCT/FAPESP).
386
387
388
389
390
391
392
393
394
395
396
397
398

References

1 A. Panacek, R. Prucek, J. Hrbac, T. Nevecna, J. Steffkova, R. Zboril, L. Kvitek, *Chem. Mater.*, 2014, **26**, 1332-1339.

2 A. Gangula, R. Podila, L. Karanam, C. Janardhana, A. M. Rao, *Langmuir*, 2011, **27**, 15268-15274.

3 K-S. Lee, M. A. El-sayed, *J. Phys. Chem. B*, 2006, **110**, 19220-19225.

4 S. S. Ravi, L. R. Christena, N. SaiSubramanian, S. P. Anthony, *Analyst*, 2013, **138**, 4370-4377.

5 S. B. Walker, J. A. Lewis, *J. Am. Chem. Soc.*, 2012, **134**, 1419-1421.

6 E. P. Hoppmann, W. W. Yu, I. M. White, *Methods*, 2013, **63**, 219-224.

7 A. Taglietti, Y. A. Diaz Fernandez, E. Amato, L. Cucca, G. Dacarro, P. Grisoli, V. Necchi, P. Pallavicini, L. Pasotti, M. Patrini, *Langmuir*, 2012, **28**, 8140- 8148.

8 P. Sanpui, A. Chattopadhyay, S. S. Ghosh, *ACS Appl. Mater. Interfaces*, 2011, **3**, 218-228.

9 M. A. Shenashen, S. A. El-Safty, E. A. Elshehy, *Part. Part. Syst. Charact.*, 2014, **31**, 293-316.

10 Y-W. Ma, Z-W. Wu, L-H. Zhang, J. Zhang, G-S. Jian, S. Pan, *Plasmonics*, 2013, **8**, 1351-1360.

11 W. L. Warnes, A. Dereux, T. W. Bobesen, *Nature*, 2003, **424**, 824-830.

12 S. Palomba, L. Novotny, R. E. Palmer, *Optics Commun.,* 2008, **281**, 480-483.

13 A. Crut, P. Maioli, N. Del Fatti, F. Vallee, *Chem. Soc. Rev.*, 2014, **43**, 3921-3956.

14 A. Querejeta-Fernández, G. Chauve, M. Methot, J. Bouchard, E. Kumacheva, *J. Am. Chem. Soc.,* 2014, **136**, 4788-4793.

15 G. Baffou, R. Quidant, *Chem. Soc. Rev.*, 2014, **43**, 3898-3907.

16 N. Cathcart, V. Kitaev, *Nanosclae*, 2012, **4**, 6981-6989.

17 Y. Xiong, Y. Xia, *Adv. Mater.*, 2007, **19**, 3385-3391.

18 N. G. Bastus, J. Comenge, V. Puntes, *Langmuir*, 2011, **27**, 11098-11105.

19 Y. Yu, K. Zhang, Q. Yao, J. Xie, J. Y. Lee, *Chem. Mater.*, 2013, **25**, 4746-4756.

20 L. Maretti, P. S. Billone, Y. Liu, J. C. Scaiano, *J. Am. Chem. Soc.*, 2009, **131**, 13972-13980.

21 A. Bankara, B. Joshi, A. R. Kumara, S. Zinjarde, *Colloids and Surfaces A: Physicochem. Eng. Aspects*, 2010, **368**, 58-63.

22 S. Kaviya, J. Santhanalakshmi, B. Viswanathan, J. Muthumary, K. Srinivasan, K. *Spectrochim. Acta Part A*, 2011, **79**, 594-598.

23 S. Singh, J. P. Saikia, A. K. Buragohain, *Colloids and Interfaces B*, 2013, **102**, 83-85.

24 Y. Zhang, G. Gao, Q. Qian, D. Cui, *Nanosclae Res. Lett.*, 2012, **7**, 475.

25 D. Yang, S. Chen, P. Huang, X. Wang, W. Jiang, O. Pandoli, D. Cui, *Green Chem,* 2010, **12**, 2030-2042.

26 N. Basavegowda, Y. R. Lee, *Mater. Lett.*, 2013, **109**, 31-33.

27 S. P. Dubey, M. Lahtinen, M. Sillanpaa, *Process Biochem.*, 2010, **45**, 1065-1071.

28 A. D. Brumbaugh, K. A. Cohen, S. K. St. Angelo, *ACS Sustainable Chem. Eng.*, 2014, **2**, 1933-1939.

29 M. Fan, G. F. S. Andrade, A. G. Brolo, *Anal. Chim. Acta*, 2011, **693**, 7-25.

30 H. Wei, H. Xu, *Nanoscale*, 2013, **5**, 10794-10805.

31 M. Wuithschick, B. Paul, R. Bienert, A. Sarfraz, U. Vainio, M. Sztucki, R. Kraehnert, P. Strasser, K. Rademann, F. Emmerling, J. Polte, *J. Chem. Mater.*, 2013, **25**, 4679-4689.

32 K. J. Major, C. De, S. O. Obare, *Plasmonics*, 2009, **4**, 61-78.

33 T. Teranishi, M. Eguchi, M. Kanehara, S. Gwo, *J. Mater, Chem.*, 2011, **21**, 10238-10242.

34 M. Sackmann, A. Materny, *J. Raman Spectrosc.*, 2006, **37**, 305-310.

35 E. B. Santos, F. A. Sigoli, I. O. Mazali, *New J. Chem.*, 2014, **38**, 5369-5375.

36 K. B. Narayanan, N. Sakthivel, *Mater. Lett.*, 2008, **62**, 4588-4590.

37 P. Rajasekharreddy, P. U. Rani, B. Sreedhar, *J. Nanopart. Res.*, 2010, **12**, 1711-1721.

38 A. B. S. Sastry, R. B. K. Aamanchi, C. S. R. L. Prasad, B. S. Murty, *Environ. Chem. Lett.*, 2013, **11**, 183-187.

39 D. Hamdan, M. Z. El-Readi, A. Tahrani, F. Herrmann, D. Kaufmann, N. Farrag, A. El-Shazly, M. Wink, *Food. Chem.*, 2011, **127**, 394-403.

40 A. Husen, K. S. Siddiqi, *Nanoscale Research Lett.*, 2014, **9**, 229-252.

41 A. Henglein, *Chem. Phys. Lett.*, 1989, **154**, 473-476.

42 T. Linnert, P. Mulvaney, A. Henglein, H. Weller, *J. Am. Chem. Soc.*, 1990, **112**, 4657-4664.

43 D. Singha, N. Barman, K. Sahu, *J. Colloid. Interface. Sci.*, 2014, **413**, 37-42.

44 V. V. Tatarchuk, A. I. Bulavchenko, I. A. Druzhinina, *Russian J. Inorg. Chem.*, 2006, **51**, 1836-1839.

45 R. Stiufiuc1, C. Iacovita, C. M. Lucaciu, G. Stiufiuc, A. G. Dutu, C. Braescu, N. Leopold, *Nanoscale Research Lett.*, 2013, **8**, 47-51.

471 46 X. Liu, Y. Cao, H. Peng, H. Qian, X. Yang, H. Zhang, *Cryst. Eng. Comm.*,
472 2014, **16**, 2365-2370.
473 47 E. C. Le Ru, P. G. Etchegoin, Principles of Surface-Enhanced Raman
474 Spectroscopy, Elsevier, Amsterdam, 2009.
475 48 A. Klinkova, R. M. Choueiri, E. Kumacheva, *Chem. Soc. Rev.*, 2014, **43**, 3976-
476 3991.
477 49 E. B. Santos, F. A. Sigoli, I. O. Mazali, *Vib. Spectrosc.*, 2013, **68**, 246-250.
478 50 S. Chen, P. Huang, Z. Wang, Z. Wang, M. Swierczewska, G. Niu, D. Cui, X.
479 Chen, *Nanosclae Res. Lett.,* 2013, **8**, 168.
480 51 Y. Wang, W. Ji, Z. Yu, R. Li, X. Wang, W. Song, W. Ruan, B. Zhao, Y.
481 Ozakib, *Phys. Chem. Chem. Phys.*, 2014, **16**, 3153-3161.
482 52 M. Fan, A. G. Brolo, *Phys. Chem. Chem. Phys.*, 2009, **11**, 7381-7389.
483 53 E. B. Santos, E. C. N. L. Lima, C. S. Oliveira, F. A. Sigoli, I. O. Mazali, *Anal.*
484 *Methods*, 2014, **6**, 3564-3568.
485 54 S. Panigrahi, S. Praharaj, S. Basu, S. K. Ghosh, S. Jana, S. Pande, T. Vo-Dinh,
486 H. Jiang, T. Pal, *J. Phys. Chem. B*, 2006, **110**, 13436-13444.

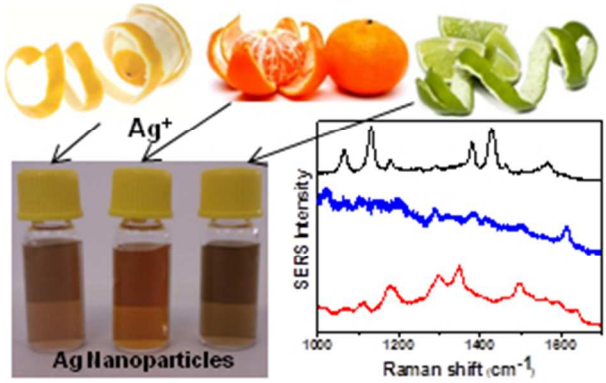

Plasmonic silver nanoparticles synthesized using citrus peel extracts exhibit SERS activity for different Raman probe molecules.
79x50mm (96 x 96 DPI)